



Effect of P on glass forming ability, magnetic properties and oxidation behavior of FeSiBP amorphous alloys



Chengjuan Wang^{a, b}, Aina He^{b, c}, Anding Wang^{b, c, *}, Jing Pang^a, Xiaofeng Liang^{a, b},
Qingfeng Li^a, Chuntao Chang^{b, c, **}, Keqiang Qiu^{a, ***}, Xinmin Wang^{b, c}

^a College of Material Science and Engineering, Shenyang University of Technology, No.111 Shenliao West Road, Economic Development District, Shenyang, Liaoning 110870, China

^b Key Laboratory of Magnetic Materials and Devices, Ningbo Institute of Materials Technology and Engineering, Chinese Academy of Sciences, Ningbo, Zhejiang 315201, China

^c Zhejiang Province Key Laboratory of Magnetic Materials and Application Technology, Ningbo Institute of Materials Technology and Engineering, Chinese Academy of Sciences, Ningbo 315201, China

ARTICLE INFO

Article history:

Received 12 August 2016

Received in revised form

24 November 2016

Accepted 30 December 2016

Available online 26 January 2017

Keywords:

Amorphous metals
Glass-forming ability
Magnetic properties
Oxidation

ABSTRACT

The effect of P on the glass forming ability, soft magnetic properties and oxidation behavior of Fe₇₈B₁₃Si_{9-x}P_x (x = 0–7) amorphous alloys were investigated. It is found that the proper introduction of P, can effectively improve the glass forming ability and stability of supercooled liquid region. Fe₇₈Si₄B₁₃P₅ BMG, which exhibits high saturation flux density of 1.56 T, was readily made into rod sample with a diameter of 1.5 mm under air casting atmosphere. P bearing alloys also exhibit excellent soft magnetic properties containing low coercivity of 1.7–2.7 A/m, and high effective permeability of 8200–12,200. Slight oxidation can further improve the coercivity to a lower value of 1.1 A/m and the higher effective permeability to 11,900 for the alloys with P content no more than 3 at. %. Excessive addition of P may deteriorate the glass forming ability, soft magnetic properties and oxidation behavior. Magnetic domain revealing the magnetization process of the amorphous ribbons were characterized to explain the effect of P on magnetic properties and oxidation behavior.

© 2017 Elsevier Ltd. All rights reserved.

1. Introduction

Fe-based amorphous alloys, characterized with low coercivity (H_c), high effective permeability (μ_e), high saturation magnetic flux density (B_s) and low core loss in a wide frequency range for free of grain boundaries [1–3], can prompt the miniaturization and high efficiency of electronic components which are important for saving energy and reducing greenhouse gas emissions. In order to meet the magnetic property and shape requirements, a large number of

Fe-based amorphous alloys have been developed [4–6]. The Fe-Si-B alloy ribbon with high B_s of 1.56 T has been widely used in devices such as transformer, choke and sensors [7,8]. The alloys with high glass forming ability (GFA) developed by adding large atom size metal elements containing Ga, Nb, Mo, Y [9–11], can be casted into bulk samples or atomized into powers. The B_s and GFA respectively depended on the Fe content and glass forming elements seem to be on two side of the balance, this limits the application of these alloys. In recent years, three metal element free systems exhibiting combined high GFA for bulk samples, high B_s , and low raw material cost were developed, containing Fe-Si-B-P, Fe-Si-B-P-C and Fe-P-C [12–14]. These P contained alloys are really attractive both for the application and for the further understanding of glass forming mechanism. However, the pronounced GFA improvement of the alloys with P partial substitution, compared with the well-studied Fe-Si-B alloys, cannot be explained convincingly by using the empirical rules like large atomic size mismatch, high mixing entropy and microstructure complexity of initial crystallization phases [15]. The influence of P content on the soft magnetic properties after annealing induced stress release and structure relaxation is

* Corresponding author. Key Laboratory of Magnetic Materials and Devices, Ningbo Institute of Materials Technology and Engineering, Chinese Academy of Sciences, Ningbo, Zhejiang 315201, China.

** Corresponding author. Key Laboratory of Magnetic Materials and Devices, Ningbo Institute of Materials Technology and Engineering, Chinese Academy of Sciences, Ningbo, Zhejiang 315201, China.

*** Corresponding author. College of Material Science and Engineering, Shenyang University of Technology, No.111 Shenliao West Road, Economic Development District, Shenyang, Liaoning 110870, China.

E-mail addresses: anding@nimte.ac.cn (A. Wang), ctchang@nimte.ac.cn (C. Chang), kqniu@163.com (K. Qiu).

also not thoroughly clear. It is thus necessary to do in-depth study of the P addition effects.

Apart from the compositional dependences of GFA and magnetic properties which are very important in actual production process and application, the oxidation behavior in annealing process which relieves the residual stresses resulting from the casting and winding processes, has also been proved to be very important in effecting the soft magnetic properties [16]. Simply, slight oxidation will increase the surface resistance and hence decrease the core loss. On the other hand, excessive oxidation will introduce a strong pinning effect [17]. For most industrial production processes, a high vacuum annealing environment is not preferred and the oxidation is always controlled by protective atmosphere simply. In many cases, the big cores are taken out of the furnace for a faster cooling rate. As proved that the oxidation depends on the compositions and the density of the oxidation products [18,19], the study of the oxidation behavior and its effect on soft magnetic properties will be an ongoing and important issue. The effect of P addition on magnetic properties and manufacturability need further investigation.

In this study, the most representative $\text{Fe}_{78}\text{Si}_9\text{B}_{13}$ was chosen as the basic composition and the effect of P content on the GFA, soft magnetic properties and oxidation behavior of Fe-Si-B-P alloy system were systematically investigated. The optimal P content judged from different aspects was also explored. Magnetic domain analysis was also carried out to reveal the effect on the magnetization process.

2. Experimental procedures

In this experiment, $\text{Fe}_{78}\text{Si}_{9-x}\text{B}_{13}\text{P}_x$ ($x = 0, 1, 3, 5$ and 7) ingots were prepared by induction melting the mixture of pure metals of Fe (99.99 mass %), premelted Fe-P (99.9 mass %), and pure metalloid of crystal B (99.9 mass %) and Si (99.999 mass %) in an argon atmosphere. The alloy compositions represent nominal atomic percent. Amorphous and/or amorphous alloys were produced in a ribbon form by a single roller melt-spinning method and rod forms by a Cu-mold casting method in air. Ribbons with a width of about 1.3 mm and thickness of about 23–26 μm were prepared by single roller melt-spinning method at the wheel speed 40 m/s in Ar atmosphere. The amorphous structure was identified by X-ray diffraction (XRD) with $\text{Cu K}\alpha$ radiation. Thermal physical parameters including Curie temperature (T_c), glass transition temperature (T_g) and crystallization temperature (T_x) of the amorphous alloys were examined by differential scanning calorimetry (DSC) at heating rate of 0.67 K/s. The liquids temperature (T_l) was measured with a DSC by cooling the molten alloy samples at a low cooling rate of 0.067 K/s to reduce the influence of undercooling. Magnetic properties of B_s , H_c and μ_e were measured with a vibrating sample magnetometer (VSM) under an applied field of 800 kA/m, a DC B-H loop tracer under a field of 800 A/m and an impedance analyzer under a field of 1 A/m, respectively. Before measuring the magnetic properties, the ribbon samples were annealed.

Oxidation tests were performed by means of the thermogravimetric analyzer (TG) in dry air, the net flow rate of air was kept constant at 200 ml/min throughout each test, and the heating rates of the TG furnace were set at 10 K/min. The TG microbalance is sensitive within ± 0.001 mg. The ribbons were annealed in a vacuum-tube furnace with a base pressure of 5×10^{-3} Pa over a temperature range of 553 K–733 K. Other samples were exposed to dry oxygen in an open-ended quartz-tube furnace at a temperature of 673 K for 5 min, 10 min, 30 min, 60 min and 90 min. The structure of magnetic domain was characterized via the Magneto-optical Kerr Microscope. The density was measured by the Archimedeian method. All the measurements were performed at room temperature.

3. Results and discussion

Fig. 1 shows DSC curves obtained from the $\text{Fe}_{78}\text{B}_{13}\text{Si}_{9-x}\text{P}_x$ master alloys. It exhibits the melting process and the solidification process. The on-set and off-set temperatures of the melting endothermic event shown in the heating section are designated by T_m and T_{lm} . The on-set temperature of the solidification exothermic event shown in the cooling section is designated by T_{ls} . With P addition, T_m and T_{lm} gradually reduced, and the fusion enthalpies obtained from the area of the fusion peak in DSC data apparently decreased, which indicates the lower binding energy of the crystalline phases [20]. As the solidification process is quasi-static because of the low cooling rate, T_{ls} reflects the liquids temperature and undercooling [20]. The undercooling determined by the $T_{lm}-T_{ls}$ of the P_1 , P_3 , P_5 and P_7 doped alloys decrease which can be related to the structure differences between the liquid and primary solid phases.

All of the alloys were readily fabricated into ribbon samples with good surface quality and bending ductility by single roller melt-spinning method. Fig. 2 shows XRD patterns of the as-quenched

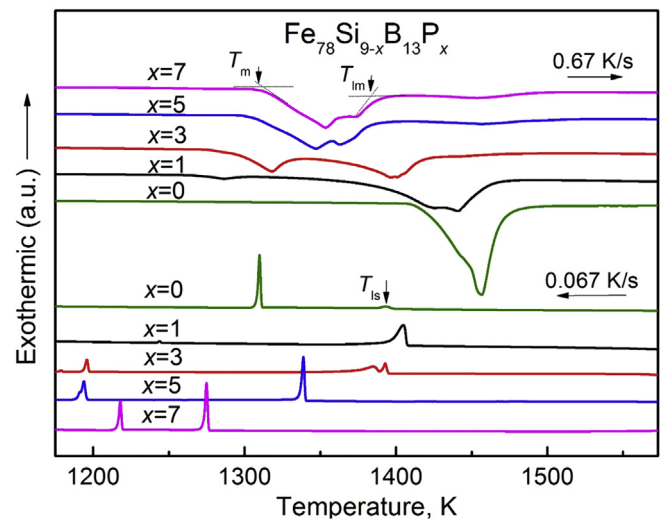


Fig. 1. DSC curves of the $\text{Fe}_{78}\text{B}_{13}\text{Si}_{9-x}\text{P}_x$ ($x = 0, 1, 3, 5$ and 7) master alloys showing the melting and solidification processes.

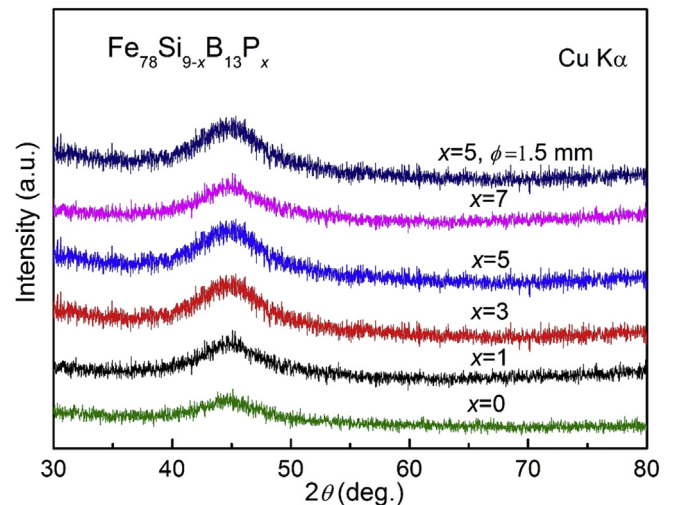


Fig. 2. XRD patterns of the $\text{Fe}_{78}\text{B}_{13}\text{Si}_{9-x}\text{P}_x$ ($x = 0, 1, 3, 5$ and 7) as-spun alloy ribbons and $\text{Fe}_{78}\text{B}_{13}\text{Si}_4\text{P}_5$ as-casted rod.

FeSiBP alloy ribbons measured from free surface. All the diffraction patterns show only one broad peak and without any detectable sharp peaks, indicating the formation of an amorphous phase in all these alloys.

The DSC curves for $\text{Fe}_{78}\text{Si}_{9-x}\text{B}_{13}\text{P}_x$ ($x = 0, 1, 3, 5$ and 7) melt-spun alloys are showed in Fig. 3. The as-spun alloys with $x = 0$ and 1 exhibit two exothermic peaks corresponding to two crystallization events, while, only one distinct crystallization exothermic peak was observed with higher P content. Moreover, the as-spun alloys with $x = 5$ exhibit a glass transition, followed by a supercooled liquid region ΔT_x ($\Delta T_x = T_x - T_g$) and then crystallization. With the P content increase from 0 to 7 at. %, T_c and T_x decrease from 688 K to 658 K, 818 K–768 K, respectively. The decrease of T_c can be explained by the weaker magnetic exchange interaction of P bearing alloys. Since the aim of annealing treatment for amorphous soft magnetic alloys is to release inner stress without crystallization or clustering [21], the annealing temperature (T_A) interval between the T_c and T_x ($T_x - T_c$) may have correlation with soft magnetic properties which needs further investigation. According to the former results of DSC measurement and thermal stability analyses, it is expected that the alloys with P content about 5 at. % may exhibit enhanced glass forming ability. The deduction was verified by the fully amorphous microstructure in Fig. 2 of the casted cylindrical rod with diameter of 1.5 mm. Compared with the well investigated $\text{Fe}_{78}\text{Si}_9\text{B}_{13}$ alloy which only can be made into ribbon sample, it is strongly confirmed that 5 at. % P element addition can effectively improve the GFA of FeSiBP alloys. Consistent with the former report [8,12], the GFA evaluating was hence not the key point in this paper.

Ribbon samples for phase evolutions and magnetic properties measurements were annealed for 10 min by isothermal furnace under a low pressure of about 5×10^{-3} Pa and the magnetic properties were then investigated systematically. Fig. 4 exhibits the annealing temperature (T_A) dependence of H_c (Fig. 4a) and μ_e (Fig. 4b) for $\text{Fe}_{78}\text{Si}_{9-x}\text{B}_{13}\text{P}_x$ ($x = 0, 1, 3, 5$ and 7) amorphous alloys annealed for 10 min. For all alloys, H_c decreases gradually with increasing T_A up to T_c , and reaches their minimum values. Consistent with P content dependence of T_c in upper DSC curves, the onset temperature of the optimal T_A range decreases with the P content increases. On the other hand, the off-set temperature determined by the upturn point increases with the increase of P

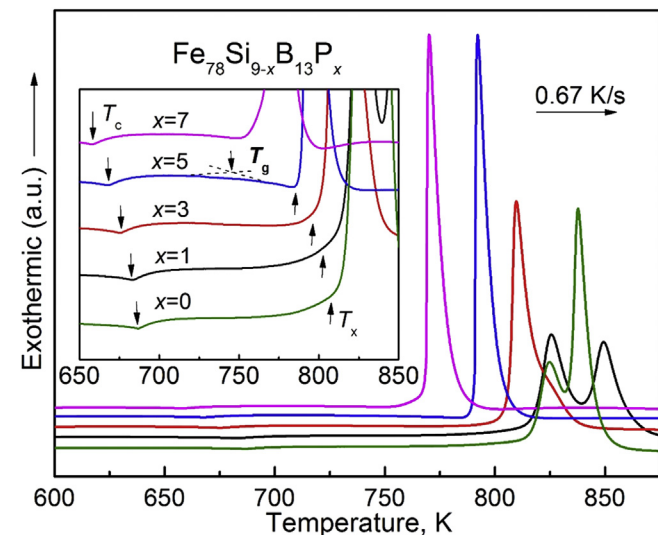


Fig. 3. DSC curves of the $\text{Fe}_{78}\text{Si}_{9-x}\text{B}_{13}\text{P}_x$ ($x = 0, 1, 3, 5$ and 7) amorphous alloys showing the crystallization behavior.

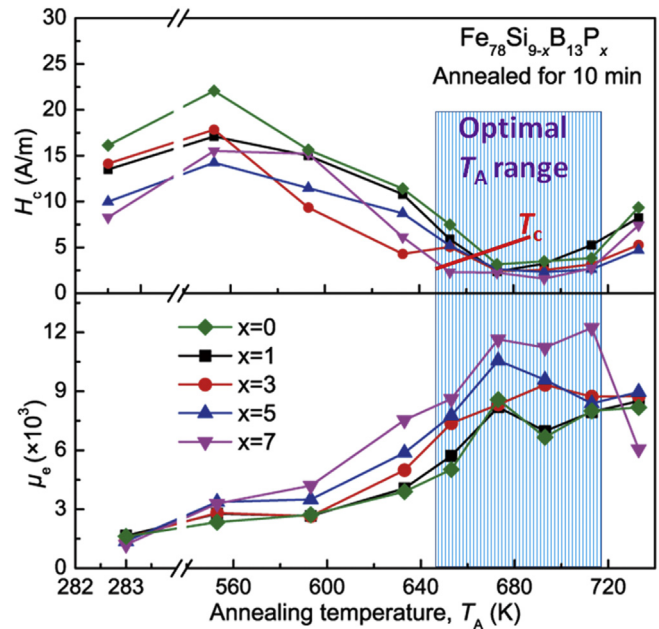


Fig. 4. Annealing temperature (T_A) dependence of H_c and μ_e for $\text{Fe}_{78}\text{B}_{13}\text{Si}_{9-x}\text{P}_x$ ($x = 0, 1, 3, 5$ and 7) amorphous alloys annealed for 10 min.

content. Consequently, the P added alloys exhibits distinctly wider optimal T_A range which are really important for the application of ferromagnetic amorphous alloys. As shown in Fig. 4b, the μ_e also reaches the peak values for the samples annealed in the optimal T_A range. In the whole, the soft magnetic properties become optimization with increase of P addition. From a structural viewpoint, the low H_c is basically understood to be originated from a formation of dense-packing structure, because the physical density increases during annealing due to structural relaxation [22]. The improvement of soft magnetic properties by P addition can be attributed to the drastically enhanced GFA and stability of supercooled liquid region, leading to high GFA and lower domain pinning center.

As shown in Fig. 5, the isochronal thermogravimetry (TG) curves of the $\text{Fe}_{78}\text{Si}_{9-x}\text{B}_{13}\text{P}_x$ ($x = 0, 1, 3, 5$ and 7) amorphous alloys tested in air at a heating rate of 10 K/min from 300 K to 1250 K were then carried out to determine the oxidation behavior. With the increase

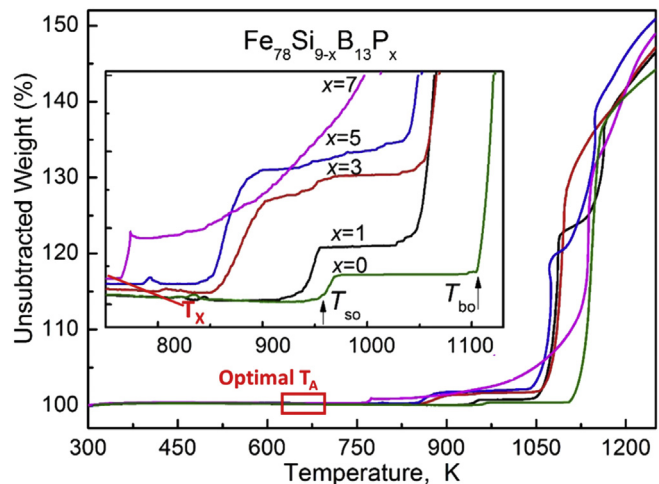


Fig. 5. The TG curves of the $\text{Fe}_{78}\text{B}_{13}\text{Si}_{9-x}\text{P}_x$ ($x = 0, 1, 3, 5$ and 7) amorphous alloys in the air atmosphere.

of P content from 0 to 7 at. %, the sensitivity of the ribbons to temperature increases, and the oxidation degree for the P added alloys at the same temperature is higher. The increase of the alloys in mass annealed at the optimal annealing T_A was very small, implying that no serious oxidation occurred. When temperature above T_x , two upturn points correlated to the distinct surface oxidation (T_{so}) occurs and body oxidation (T_{bo}) were cleared detected for all alloys. As enlarged in the insert, the steady range of TG curves between the T_{so} and T_{bo} can be explained by the protective effect of the oxidation layer on the surface of the ribbon. It is clear that T_{so} , T_{bo} and $T_{bo}-T_{so}$ decrease gradually with the increase of P content. Combinedly analyse the DSC and TG curves, we propose that: 1) T_{so} reflects the chemical activity and oxidation performance of the crystallization phase, 2) the T_{bo} and $T_{bo}-T_{so}$ changes reflect the difference of the microstructure of the oxidation layer and chemical activity of crystallization phase with different P content. The interfacial and strain energies which will be generated during the crystallization of the amorphous alloys may contribute to the higher chemical activity and more oxidatio interface [16]. When body oxidation occurs, the formation of oxide causes a reduction of the molar volume, and results in a residual tensile stress. So that a residual tensile stress may be generated in the two-oxide boundary, which in turn results in the initial cracks in the scales. Once the cracks propagate through the scales, the scale integrity is broken and the substrate is exposed to air, thereby leading to a catastrophic oxidation [23]. According to the previous reports [20], the crystallization phases of the $Fe_{78}B_{13}Si_{9-x}P_x$ ($x = 0, 1, 3, 5$ and 7) alloys are α -Fe(Si) and $Fe_3(B,P)$. With the increase of P content, the $Fe_3(B,P)$ compound are more loose and chemically active for oxidation.

Based on the upper results, the oxidation process at the optimal T_A for these alloys is not so fast, which makes it possible to anneal the samples in air or oxygenic atmosphere. Apart from the T_A , it is accepted that annealing process is also affected by annealing time (t_a) and oxygen content. For $Fe_{78}B_{13}Si_{9-x}P_x$ ($x = 0, 1, 3, 5$ and 7) amorphous alloys annealed in air atmosphere, changes in H_c and μ_e as a function of t_a at optimal T_A of 673 K are shown in Fig. 6. Accordingly, we can draw three points: 1) moderate oxidation can improve the soft magnetic properties for the low P content alloys,

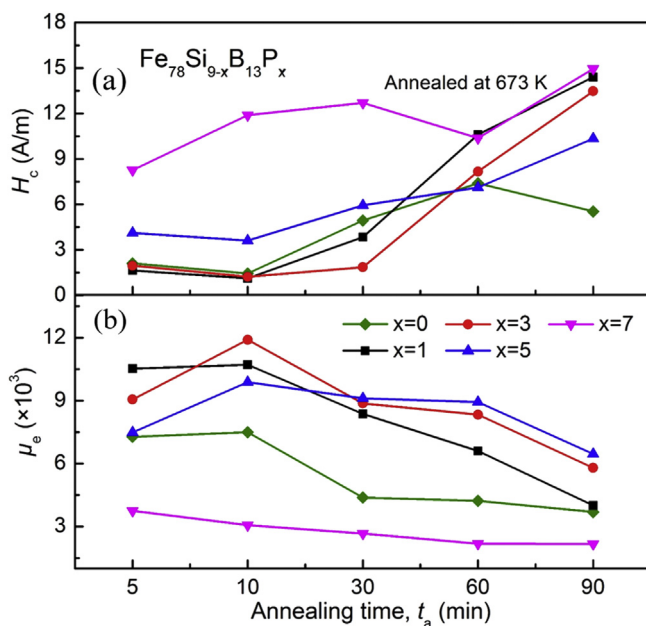


Fig. 6. Annealing time dependence of H_c and μ_e for $Fe_{78}B_{13}Si_{9-x}P_x$ ($x = 0, 1, 3, 5$ and 7) amorphous alloys annealed in the air atmospheres at 673 K.

2) excessive oxidation deteriorates the soft magnetic properties greatly, 3) the optimal t_a range becomes narrow with the increase of P content. For alloys with $x = 0, 1$ and 3 , the H_c are better than that of samples annealed in vacuum for 10 min. While for the alloys with $x = 7$, the soft magnetic properties of the samples annealed in air deteriorate. The $Fe_{78}B_{13}Si_2P_7$ alloy ribbon is more sensitive to oxygen, consistent with the results of TG. The μ_e curves also reveal the best soft magnetic properties can be obtained for the alloys with $x = 0-3$ even when annealed in air.

Then, the hysteresis magnetic loops of the amorphous ribbons annealed in different atmospheres were measured by VSM. As shown in Fig. 7, for the representative $Fe_{78}Si_4B_{13}P_5$ alloys, all loops show typical soft magnetic characteristic and the B_s of the sample annealed in air is comparatively lower. The inset (a) shows the H_c increased owing to excessive oxidation. As the illustrated in inset (b), the B_s of the alloys decreases with the increase of P content. What's more, the dropped B_s induced by serious oxidation can be clearly seen in Fig. 7, proving the higher oxidation degree of the P bearing alloys.

For further understanding the changes of soft magnetic properties, magnetic domains of the representative $Fe_{78}Si_9B_{13}$ and $Fe_{78}Si_4B_{13}P_5$ ribbon samples under different conditions were studied with Magneto-optical Kerr Microscopy. As shown in Fig. 8, the magnetic domains for sample with different state and P content exhibit quite different patterns, which can reflect the soft magnetic properties. For ribbons with as-quenched state, the magnetic domain in Fig. 8 a1 is disordered, because of the strong and non-uniform internal stress stems from the fast cooling process. According to the studies of Tejedor et al., the surface of the as quenched amorphous ribbon is in randomly distributed compressive stress which will gradually changes to tensile stress in the central part [24]. During annealing below the crystallization temperature, structural relaxation which will lead to a uniform microstructure, free volume annihilating and stress release happens, resulting in the change of domain to regular patterns (Fig. 8 a2 and b1). Comparing the stripe domain for $Fe_{78}Si_9B_{13}$ alloy and a zigzag domain for $Fe_{78}Si_4B_{13}P_5$ alloy, we can also find that the angle between ribbon and domain directions changes from perpendicular to small value, which can be used to explain the important of soft magnetic properties by P addition [25]. For the samples with excessive oxidation represented in Fig. 8 b2, domain

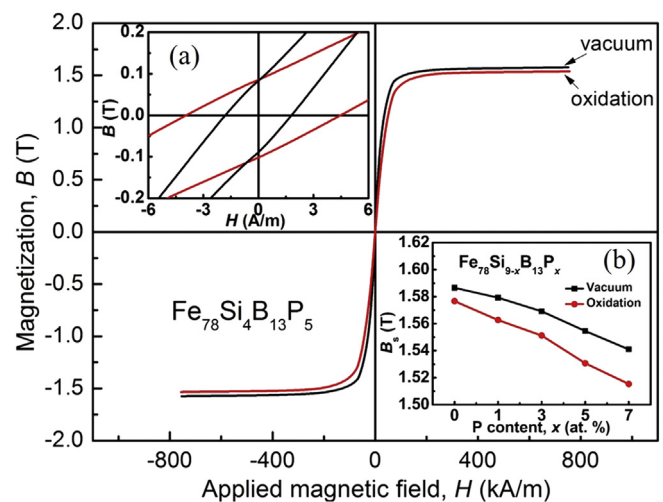


Fig. 7. Hysteresis loops measured with VSM, B - H loops (inset a) measured with B - H loop tracer of melt-spun amorphous alloy $Fe_{78}B_{13}Si_4P_5$ and B_s values of $Fe_{78}B_{13}Si_{9-x}P_x$ ($x = 0, 1, 3, 5$ and 7) amorphous alloys (inset b) annealed under vacuum and in the air atmospheres at 673 K, respectively.

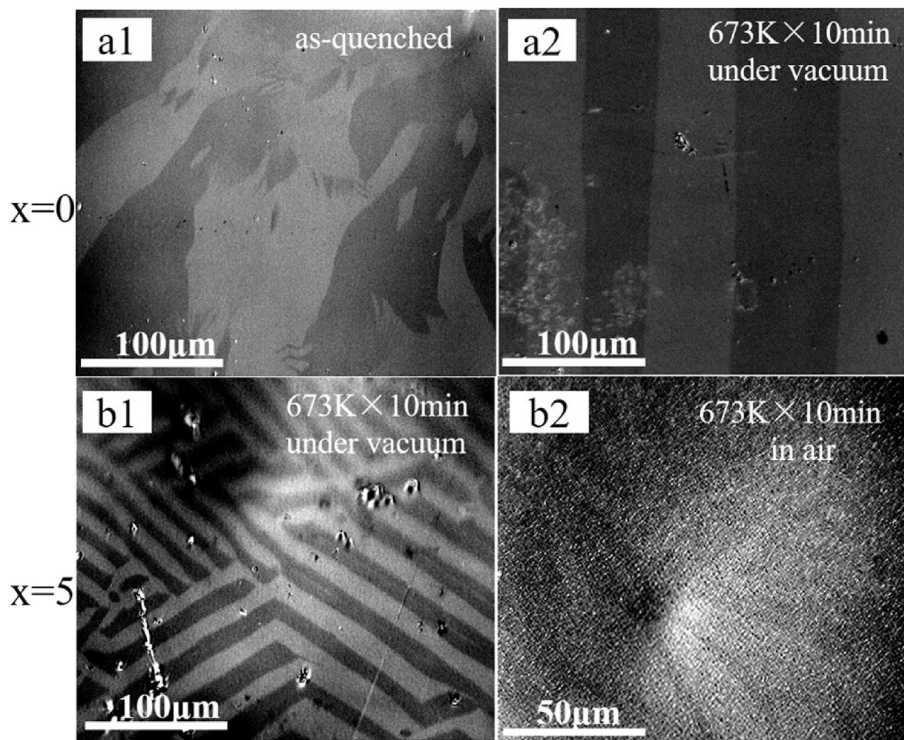


Fig. 8. Typical magnetic domains of $\text{Fe}_{78}\text{B}_{13}\text{Si}_{9-x}\text{P}_x$: $x = 0$ and 5 alloy ribbons.

morphology cannot be clearly observed for $\text{Fe}_{78}\text{Si}_4\text{B}_{13}\text{P}_5$ alloy because of the formation of surface oxide layer. Although an important feature of amorphous alloys is, furthermore, the absence of any grain or phase boundaries which are known to act as strong pinning centers for domain walls in crystalline materials [26], the existence of the oxide layer formation can cause tensile stresses in the amorphous matrix, as main pinning source.

Taking into account all experimental findings, the effect of P addition can be summarized and we will try to explore the mechanism from the following aspects. First, we focus on the pronounced effect of P addition on increasing the GFA. The mixing enthalpies of Fe and Si, B, P pairs are -18 , -11 and -31 kJ/mol, respectively [20]. The mixing enthalpy can be enlarged by partially substituting Si with P. It is proved that large negative mixing enthalpies between the constituent elements lead to a highly stable supercooled liquid. As shown in Fig. 1, the addition of P drastically decreases the T_m , T_{1m} and the fusion enthalpies which means that the alloys are more close to the eutectic point. The addition of P will also make the crystallization phases more complicated. All of these changes will lead to an enhanced GFA.

Then we discuss the effect on soft magnetic properties. Chen et al. have pointed out that the electrons transfer from the metalloid elements to fill the d shells in the transition metal elements Fe and then an $s-d$ hybrid bonding is formed in amorphous alloys. Since P has stronger interaction with Fe than B and Si [27], we can deduce that the $s-d$ hybrid bonding nature in P bearing alloys would become stronger. According to Das's reports, the improved thermal stability and magnetic properties can be explained by atomic interactions and $s-d$ hybridization between the ferromagnetic metal and the metalloid atoms [28,29]. The effect of the P addition on B_s should be explain from two angles. For the samples with neglectable oxidation annealed in vacuum, the P addition induced decrease of B_s is attributed to the decrease of d orbit electrons. For the samples with oxidation, the higher oxidation degree of the high P content alloys is the key reason for the decrease of B_s . The

improvement of soft magnetic containing H_c and μ_e can be attributed to the enhanced GFA and higher stability of amorphous alloys. The glass transition in Fig. 3 of the alloys with proper addition of P indicates the higher amorphicity and lower density of clusters or precipitations [12]. Another reason is the sufficient release of stress during annealing treatment at the optimal temperature. The structural and chemical homogeneity will greatly decrease the density of the domain-wall pinning sites.

The P content dependence of oxidation behavior should be explained from the chemical activity. Compared with the Si and B, P has distinctly higher chemical activity. The Fe-Si-B-P alloy system becomes more sensitive to the oxygen, consistent with the magnetic domain test results in Fig. 8. Thus, it is necessary to develop new annealing process for its future application. It should be emphasized that proper oxidation at the surface can decrease the surface pinning centers which improve the soft magnetic properties. We can improve the soft magnetic properties by tuning the oxidation degree in the future.

4. Conclusion

By adjusting P content, $\text{Fe}_{78}\text{B}_{13}\text{Si}_{9-x}\text{P}_x$ ($x = 0, 1, 3, 5$ and 7) amorphous alloys were prepared. Effects of P on glass forming ability, magnetic properties and oxidation behavior of FeSiBP amorphous alloys were investigated. The main conclusions are as follows:

- 1) We confirm the suitable addition of P can effectively enhance the GFA of FeSiB alloys, while excessive P addition deteriorates the GFA. $\text{Fe}_{78}\text{Si}_4\text{B}_{13}\text{P}_5$ amorphous alloy exhibits obvious supercooled liquid region of 60 K and the rod-specimen with diameter up to 1.5 mm was readily formed.
- 2) The P containing alloys exhibit excellent soft magnetic properties containing low H_c of 1.7–3.0 A/m, high μ_e of 81,00–11,600

and high B_s of 1.59–1.54 T after annealing at 673 K for 10 min under vacuum.

- 3) The P addition greatly decrease the anti-oxidation ability and B_s of the alloys annealed under vacuum. The alloys with P content of ≤ 3 at. % can reach the optimal soft magnetic properties by annealing in air.
- 4) Moderate oxidation can further improve the soft magnetic properties of low P content alloys. The alloys with P content of ≤ 3 at. % and moderate oxidation exhibit better magnetic properties, which exhibit low H_c of 1.1–1.4 A/m, high μ_e of 11,900–10,700.

Acknowledgement

This work was supported by the National Natural Science Foundation of China (Grant No. 51541106), Ningbo International Cooperation Projects (Grant No. 2015D10022), Ningbo Major Project for Science and Technology (Grant No. 2014B11012), Shenyang Science And Technology Project (F14-231-1-22).

References

- [1] M.E. McHenry, M.A. Willard, D.E. Laughlin, Amorphous and nanocrystalline materials for applications as soft magnets, *Prog. Mater. Sci.* 44 (1999) 291–433.
- [2] Santanu Das, Reinaldo Santos-Ortiz, Electromechanical behavior of pulsed laser deposited platinum-based metallic glass thin films, *Phys. Status Solidi A* 213 (No. 2) (2016) 399–404.
- [3] Medha Veligatla, Santanu Das, Junyeon Hwang, Tuning the magnetic properties of cobalt-based metallic glass nanocomposites, *JOM-US* 68 (No. 1) (2016) 336–340.
- [4] Y.I.a.Y.E.K. Yamada, The magnetic phase transition of an amorphous Fe-P-C and its alloys containing Ni and Cr, *Solid State Commun.* 16 (1975) 1335–1338.
- [5] J. Durand, Concentration dependence of the magnetic properties in amorphous Fe-P-B alloys, *IEEE Trans. Magn.* 12 (1976) 945–947.
- [6] M. Mittra, T. Masumoto, N.S. Kazama, Effect of silicon addition on the magnetic properties of Fe-B-C amorphous alloys, *J. Appl. Phys.* 50 (1979) 7609.
- [7] D. Arvindha Babu, B. Majumdar, A.P. Srivastava, B. Ramakrishna Rao, D. Srivastava, B.S. Murthy, D. Akhtar, Structure, properties, and glass forming ability of melt-spun Fe-Zr-B-Cu alloys with different Zr/B ratios, *Metall. Mater. Trans. A* 42 (2010) 508–516.
- [8] M. Aykol, M.V. Akdeniz, A.O. Mekhrabov, Solidification behavior, glass forming ability and thermal characteristics of soft magnetic Fe-Co-B-Si-Nb-Cu bulk amorphous alloys, *Intermetallics* 19 (2011) 1330–1337.
- [9] A. Makino, A. Inoue, T. Mizushima, Soft magnetic properties of Fe-based bulk amorphous alloys, *Mater. T. JIM* 41 (2000) 1471–1477.
- [10] H. Koshiba, A. Inoue, A. Makino, Fe-based soft magnetic amorphous alloys with a wide supercooled liquid region, *J. Appl. Phys.* 85 (1999) 5136.
- [11] O. Haruyama, H.M. Kimura, A. Inoue, Thermal stability of Zr-based glassy alloys examined by electrical resistance measurement, *Mater. T. JIM* 37 (1996) 1741–1747.
- [12] A. Makino, C.T. Chang, T. Kubota, A. Inoue, Soft magnetic Fe-Si-B-P-C bulk metallic glasses without any glass-forming metal elements, *J. Alloy. Compd.* 483 (2009) 616–619.
- [13] A. Makino, T. Kubota, C.T. Chang, M. Makabe, A. Inoue, FeSiBP bulk metallic glasses with unusual combination of high magnetization and high glass-forming ability, *Mater. Trans.* 48 (2007) 3024–3027.
- [14] Z.K. Zhao, C.T. Chang, A. Makino, A. Okubo, A. Inoue, Preparation of bulk glassy Fe₇₆Si₉B₁₀P₅ as a soft magnetic material by spark plasma sintering, *Mater. Trans.* 50 (2009) 487–489.
- [15] A.D. Wang, Q.K. Man, M.X. Zhang, H. Men, B.L. Shen, S.J. Pang, T. Zhang, Effect of B to P concentration ratio on glass-forming ability and soft-magnetic properties in [(Fe_{0.5}Ni_{0.5})_{0.78}BO_{0.22-x}P_x]₁₉₇Nb₃ glassy alloys, *Intermetallics* 20 (2012) 93–97.
- [16] K.R. Lim, J.M. Park, S.J. Kim, E.-S. Lee, W.T. Kim, A. Gebert, J. Eckert, D.H. Kim, Enhancement of oxidation resistance of the supercooled liquid in Cu-Zr-based metallic glass by forming an amorphous oxide layer with high thermal stability, *Corros. Sci.* 66 (2013) 1–4.
- [17] F. Reichel, L.P.H. Jeurgens, E.J. Mittemeijer, The thermodynamic stability of amorphous oxide overgrowths on metals, *Acta Mater.* 56 (2008) 659–674.
- [18] W. Kai, I.F. Ren, R.F. Wang, C.T. Liu, The oxidation behavior of an Fe₆₁B₁₅Zr₈-Mo₇Co₅Y₂Cr₂ bulk metallic glass at 650°C in various oxygen-containing environments, *Intermetallics* 17 (2009) 165–168.
- [19] M. Josefina, A. Silveyra, Emilia Illeková, Effects of air annealing on Fe-Si-B-M-Cu (M = Nb, Mo) alloys, *J. Alloys Compd.* 610 (2014) 180–183.
- [20] A.D. Wang, C.L. Zhao, A.N. He, H. Men, C.T. Chang, X.M. Wang, Composition design of high Bs Fe-based amorphous alloys with good amorphous-forming ability, *J. Alloys Compd.* 656 (2016) 729–734.
- [21] I.B. Kekalo, P.S. Mogil'nikov, Relaxation of bending stresses and the reversibility of residual stresses in amorphous soft magnetic alloys, *J. Exp. Theor. Phys.* 120 (2015) 982–988.
- [22] A. Makino, T. Kubota, C.T. Chang, M. Makabe, A. Inoue, FeSiBP bulk metallic glasses with high magnetization and excellent magnetic softness, *J. Magn. Mater.* 320 (2008) 2499–2503.
- [23] N. Hua, L. Huang, J. Wang, Y. Cao, W. He, S. Pang, T. Zhang, Corrosion behavior and in vitro biocompatibility of Zr-Al-Co-Ag bulk metallic glasses: an experimental case study, *J. Non-Cryst. Solids* 358 (2012) 1599–1604.
- [24] J.A.G.A.M. Tejedor, J. Carrizo, L. Elbaile, Mechanical determination of internal stresses in as-quenched magnetic amorphous metallic ribbons, *J. Mater. Sci.* 32 (1997) 2337–2340.
- [25] C.L. Zhao, A.D. Wang, A.N. He, S.Q. Yue, C.T. Chang, X.M. Wang, R.W. Li, Correlation between soft-magnetic properties and $T_{X1}-T_c$ in high B_s FeCoSiBPC amorphous alloys, *J. Alloys Compd.* 659 (2016) 193–197.
- [26] K. Weller, T. Suter, Z.M. Wang, L.P.H. Jeurgens, E.J. Mittemeijer, The effect of pre-oxidation treatment on the corrosion behavior of amorphous Al_{1-x}Zr_x solid-solution alloys, *Electrochim. Acta* 188 (2016) 31–39.
- [27] H.S. Chen, Correlation between elastic constants and flow behavior in metallic glasses, *J. Appl. Phys.* 49 (1978) 462.
- [28] Santanu Das, Kamal Choudhary, Aleksandr Chernatynskiy, Spin-exchange interaction between transition metals and metalloids in soft-ferromagnetic metallic glasses, *J. Phys. Condens. Matter* 28 (2016), 216003 (9pp).
- [29] Medha Veligatla, Shravana Katakam, Santanu Das, Effect of iron on the enhancement of magnetic properties for cobalt-based soft magnetic metallic glasses, *Metall. Mater. Trans. A* 46A (2015) 3.